# A Rapid Compression-Expansion Machine: The experimental setup and first results with DME-air mixtures

M. Werler*, R. Schießl, U. Maas

Institute of Technical Thermodynamics, Karlsruhe Institute of Technology

**Abstract**

A Rapid Compression-Expansion Machine (RCEM) was developed. The RCEM allows operation like an RCM, with the additional option of freezing ongoing chemical reactions in the compressed cylinder load by rapid expansion. A detailed description of the experimental setup is given. First ignition delay times of DME-air-mixtures obtained with the RCEM are shown. They agree well with literature data from other RCMs. GC-analyses of the partially reacted exhaust gas are presented, providing additional data for mechanism development and validation.

## Introduction

For a long time rapid compression machines (RCM) have been used to investigate reaction kinetics and they are becoming increasingly popular as instruments for investigating auto-ignition chemistry [1-6]. The main focus on measurements with RCMs is the ignition delay time for a given fuel-air mixture at a given pressure- and temperature trajectory. There are a lot of different designs and functionalities of rapid compression machines [1-6]. The purpose of this paper is to introduce the reconditioned RCM which was previously described in [7].

While ignition delay time is an important quantity for validation of chemical reaction mechanisms [8], the validation can be rendered more rigorous if additional detailed information about the ignition process, like for instance, species time profiles, are available [9]. To extend the capability of the RCM [7] in this respect, the whole concept was revised and additional measurement systems were installed.

Application of these facilities is demonstrated for investigating dimethyl ether (DME). There is a huge interest in using DME as an ignition enhancer or as an alternative fuel [10-12]. Numerous studies on the chemical kinetics of DME in several experimental setups were already conducted. A study on the oxidation of DME in a jet stirred reactor was published by Dagaut et al. [12]. They measured concentration profiles of reactants, intermediates and products covering a wide range of conditions [12]. Fischer et al. measured species concentrations for the pyrolysis and oxidation of DME in flow reactors and compared them to a detailed chemical kinetic mechanism [13, 14]. Studies on DME-air flames at atmospheric pressure were conducted by Kaiser et al. Chemical species profiles were measured by gas chromatography or Fourier transform infrared spectroscopy [15]. Ignition delay times of stoichiometric DME-air mixtures were measured in a shock tube by Pfahl et al. [16]. All these experimental data [12-16] were used to validate the DME reaction mechanism developed by LLNL [13-15].

Another DME reaction mechanism was developed by Zhao et al. [17]. The mechanism was compared to a variable pressure flow reactor [17]. In addition to that this mechanism was compared to rapid compression measurements by Mittal et al. [18]. Ignition delay times were measured for diluted mixtures in the region of negative temperature coefficient behavior for equivalence ratios of 0.43-1.5 and a pressure of 10-20 bar [18].

Recently Burke et al. published a study on ignition delay time measurements in a rapid compression machine and a shock tube for DME-air and DME-methane-air mixtures [19]. They investigated DME-air mixtures at equivalence ratios of 0.3 – 2 and for pressures ranging from 7-41 bar in a wide temperature range ($T$ = 600–1600 K) [19]. A new DME/methane reaction mechanism was developed and compared to the measurements [19] together with the mechanisms developed by LLNL [13-15] and Zhao et al. [17].

Furthermore DME-air mixtures were investigated in a shock tube by Cook et al. They measured ignition delay times for temperatures above 1175 K, equivalence ratios from 0.5 to 3 and for pressures up to 6.6 bar [20]. The observed data were compared to simulations based on the mechanism by LLNL [13-15] and by Zhao et al. [17].

In addition to the mixtures of DME with ethane Zhang et al. measured ignition delay times of pure DME-air mixtures at pressures of 2 and 20 atm at equivalence ratios ranging from 0.5 to 2 and temperatures of 1100-1500 K [21]. The Zhao et al. [17] mechanism was compared to these measurements [21].

This extensive availability of measurement data and reaction mechanisms made DME-air mixtures a good base to test the revised experimental setup. At one go the collected data widen the investigated temperatures of undiluted DME-air mixtures at equivalence ratios of 1 and 2 to lower temperatures.

## Rapid Compression-Expansion Machine (RCEM)

The RCM which was used as basis for the RCEM development was previously explained in [7]. Fig. 1 shows the schematic construction of the revised RCEM. It consists of a temperature controlled cylinder-piston device. A creviced piston is used to swallow the boundary layer peeled off the cylinder wall during the compression. This shall contribute a more homogeneous temperature field in the reaction chamber.

* Corresponding author: marc.werler@kit.edu

The cylinder head is equipped with a quartz pressure transducer (Kistler 6061 B) to record time-resolved the in-cylinder pressure traces. The pre-compression pressure is measured by an absolute pressure gauge (MKS Baratron 121A). Combining both pressure sensors makes it possible to determine the absolute pressure. To measure the pre-compression temperature a type K thermocouple is used. Furthermore, the cylinder head is equipped with an optical access (quartz glass window) and an optical-fiber. Using a photomultiplier along with a dichroic short pass filter (cutoff wavelength 450 nm), a time-resolved detection of chemiluminescence emissions is possible. During the measurement a potentiometric position sensor (Burster type 7812) is applied to record the piston position.

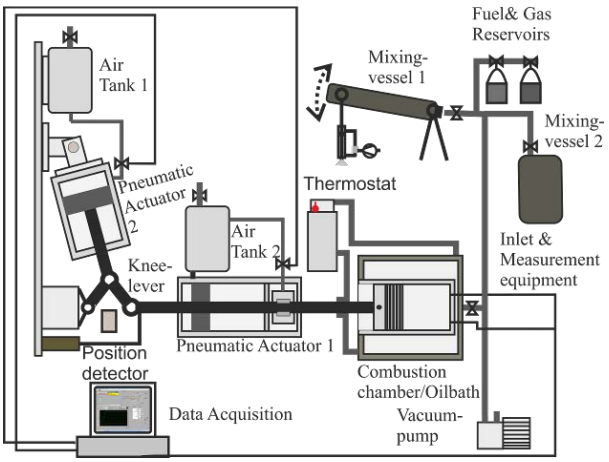

Fig. 1: Schematic construction of the RCEM

In addition to the in-cylinder measurement systems, two devices for ex-situ measurements are applied to the RCM. Absorption spectra of the test gas can be measured in a glass cell, which is connected to the reaction chamber via a fast magnetic valve. The measurement system consists out of a deuterium light source (Ocean Optic D2000) supplying continuous radiation in the region from 200 to 450 nm) and a UV-VIS spectrograph (Ocean Optic USB4000). A more detailed analysis of the test gas is possible with a micro gas-phase chromatograph (Agilent 490 Micro GC). The micro GC is equipped with 3 chromatography columns, namely a MS5A, PPU and a 5CB, allowing the analysis of permanent gases as well as many hydrocarbons up to a number of 10 carbon atoms.

Two mixing vessels are connected to the RCEM, which create and store a homogeneous mixture. To avoid density stratification, mixing vessel 1 is periodically moved around the horizontal axis, fording a Teflon ball rolling inside the chamber from one side to the other, thus continuously stirring the mixture. For the same reason, mixing vessel 2 is equipped with a magnetically coupled stirrer system. The piping system and vessel no. 2 are wrapped with electrical heating mats to enable storage temperatures of up to 150°C. This allows the creation of mixtures with less volatile fuels. In case of measurements with volatile substances one mixing vessel can be used to store “unreactive” mixtures to allow alternating measurements.

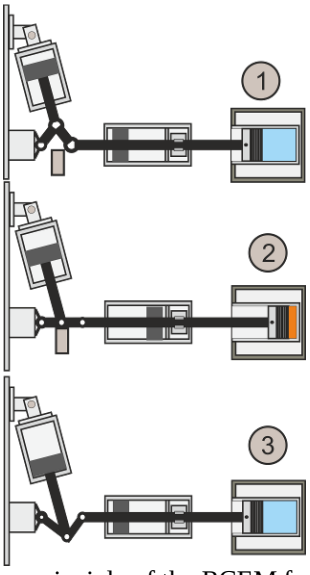

Fig. 2: Working principle of the RCEM for probe sampling by rapid expansion.

The driving section consists of pneumatic actuators, a knee-lever and a bumper. Two pneumatic actuators are connected to the driving rod, one horizontally and another almost vertical on the knee-lever hinge. Another pneumatic actuator is connected to the bumper. Buffer air tanks are connected to the actuators to ensure that the piston is driven by a nearly constant force. A pneumatic clamp prevents the driving rod from moving, even if the actuators are pressurized. By releasing the clamp off the driving rod starts the experiment and the data acquisition.

The piston is pushed into the reaction chamber either by the vertical pneumatic actuator or by a combination of the vertical and the horizontal actuators, depending on the investigated post-compression pressure. At the time the piston reaches TDC, the knee-lever hits the bumper in its elongated position and locks the piston (Fig. 2 – 2). The pneumatic actuator 2 (Fig. 1) stays pressurized. After the piston has been locked, the bumper can be removed at any time using a third pneumatic actuator. This leads to a deflection of the knee-lever and the piston is pulled out of the reaction chamber by the actuator 2 (Fig. 2 – 3). This leads rapidly to an expansion of the test mixture, freezing many of the ongoing chemical reactions, involving stable species.

With the revised driving system a good shot-to-shot repeatability of the RCM is observed. Fig. 3 shows the overlapping pressure traces of four experiments with an expansion at different times.

As shown in Fig. 3 the time span between the moment where the piston reaches TDC and the inflection point of the pressure trace due to ignition is defined as the ignition delay time. To assign the ignition delay time to a temperature and a pressure, the measured value of pressure at TDC (point 2 in Fig. 3) is used. With this pressure at TDC the corresponding temperature is calculated using the adiabatic core assumption, from the measured pre-compression pressure and temperature ($p_0$, $T_0$). To achieve a certain desired temperature at TDC,

the initial temperature, the compression ratio and the composition of the inert gas in the test mixture can be varied.

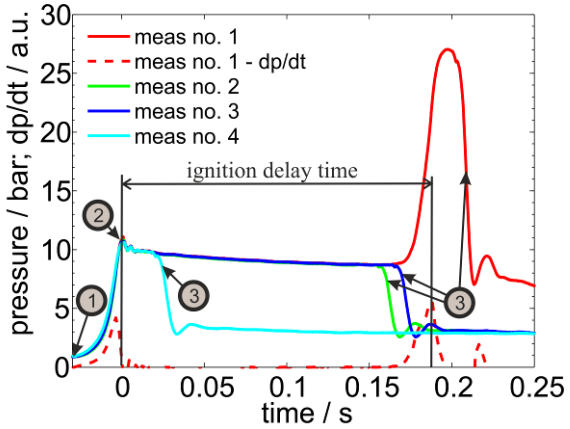


Fig. 3 Pressure traces of 4 experiments using the expansion function of the RCEM.

**Ignition Delay Times**

Ignition delay times were measured for the test gas compositions shown in Table 1. Mixture 1 and 3 were used to compare measurements of the RCEM to literature data from other RCMs. Therefore, the composition of these mixture-gases are similar to the data published by Mittal et al. [18].

Table 1 Compositions of the test gases.

| Mixture no. | 1 | 2 | 3 | 4 |
|---|---|---|---|---|
| ϕ | 0.47 | 1 | 1.47 | 2 |
| DME | 2.86 | 6.54 | 2.86 | 12.28 |
| $O_2$ | 20 | 19.63 | 5.72 | 18.42 |
| $N_2$ | 77.14 | 73.83 | 91.14 | 69.3 |

Fig. 4 compares the ignition delay times of the current study to the RCM-data of Mittal et al. for the mixture no. 1 and 2. Closed symbols represent the main ignition event, open symbols represent the first stage ignition. Measurements at an equivalence ratio of ϕ=0.47 are shown as square symbols while measurements for ϕ=1.4 are shown circles.

For the lean mixture (no. 1) an agreement between the data of the current study and the Mittal et al. [18] data is observed for the first stage ignition as well as for the main ignition. The measurements of the rich mixture overall also agree, albeit with some deviations. The first stage ignition of the literature data is slightly faster than of the current study. In the measured data of Mittal et al. [18] no or just a slight influence of the equivalence ratio can be observed for the first stage ignition delay time. The main ignition delay time shows an inverse behavior. At temperatures above 650 K the main ignition takes place somewhat faster in this study. Below 650 K the ignition delay time is longer.

A comparison with literature data [16, 19] for the mixtures no. 2 and 4 is shown in Fig. 5. The data of Burke et al. [19] was measured in a rapid compression machine and the data of Pfahl et al. [16] in a shock tube. Again the closed symbols represent the main ignition event and the open symbols represent first stage ignition delay times. All measurements were conducted at slightly differing pressures between 10 and 13 bar.

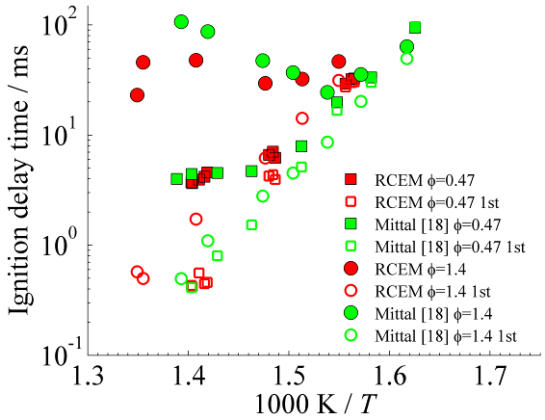


Fig. 4 Comparison of DME/air ignition delay of the current and Mittal et al. [18] study.

The ignition delay times agree well for ϕ=1. Although the pressure in the measurements of Burke et al. [19] is with 11 bar slightly higher than this of the current study, their ignition delay times are slightly longer. This effect is stronger for the higher investigated temperatures. Above a temperatures of 690 K, ignition occurred too fast in the current study to allow reliable measurements. The shock tube data are overlapping the RCEM measurements, despite its slightly higher pressure.

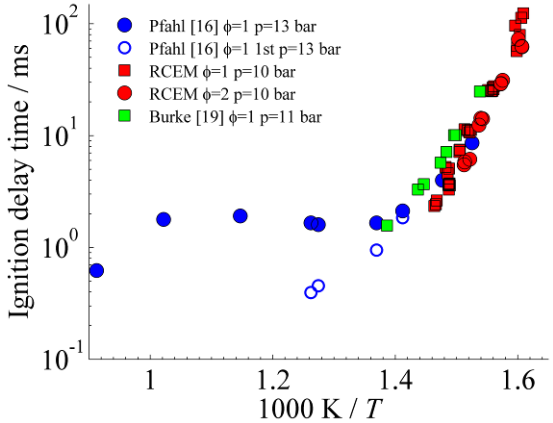


Fig. 5 Comparison of DME/air mixtures for RCEM and literature data at 10-13 bar.

**Numerical Simulations**

Numerical simulations of auto-ignition in DME/air mixtures were conducted applying a homogeneous reactor model. To account for the heat loss and the compression phase, a model described in detail by Mittal et al. [4] was used in the simulations. Two sets of simulations were conducted, based on chemical reaction

mechanisms developed by LLNL [13-15] and Zhao et al. [17] for the mixtures no. 2 and 4.

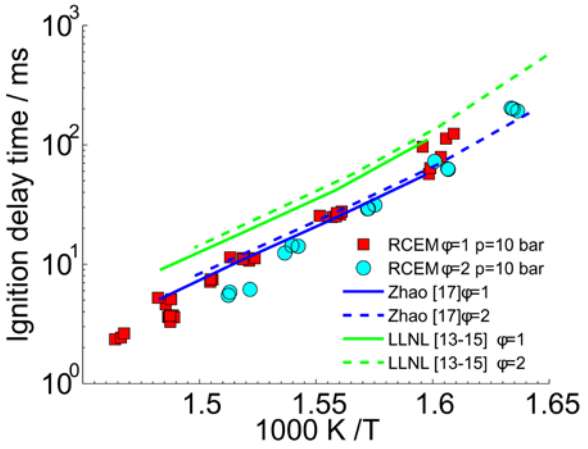


Fig. 6 Comparison of measured and simulated ignition delay times.

Figure 6 compares measurements and simulations in an Arrhenius diagram. Both mechanisms show a slightly longer ignition delay time for the mixture with a higher equivalence ratio. In contrast to that, a higher equivalence ratio leads to slightly faster ignition delay times in the measurements. The effect of temperature on the ignition delay, represented by the slope of the datasets in figure 6, is described well for both mechanisms. However, the mechanism developed by LLNL predicts slightly longer ignition delay times than observed experimentally, and also compared to simulations with the mechanism developed by Zhao et al.

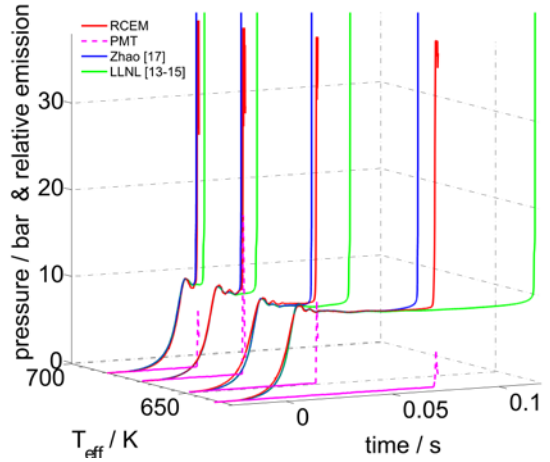


Fig. 7 Exemplary time histories of pressure traces and chemiluminescence emission for mixture no. 2; Experimental: RCEM (pressure), PMT (emission); Simulations: Zhao [17] and LLNL [13-15] (pressure).

In Figure 7, four exemplary pressure traces of the experiments are shown and compared to those predicted by numerical simulations for an equivalence ratio of $\phi = 1$. Furthermore the chemiluminescence emission signals are depicted as detected in the RCEM by a photomultiplier tube for wavelengths below 450 nm. In the pressure profiles as well as in the chemiluminescence signal no first stage ignition phenomena could be observed. The same applies to the measurements with an equivalence ratio of $\phi = 2$, shown in figure 8.
For both mechanisms and with all mixtures, a better agreement of ignition delay times is observed for the higher temperatures.

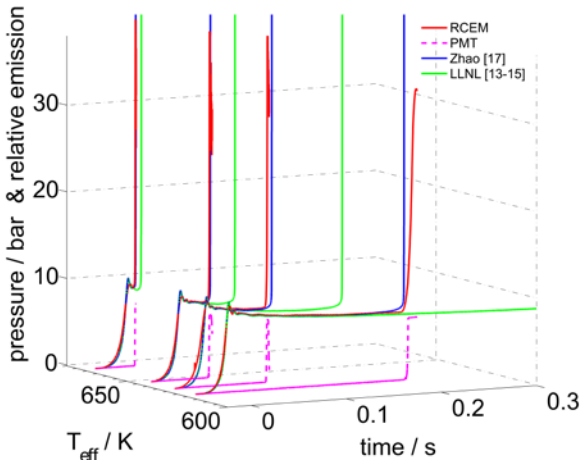


Fig. 8 Exemplary time histories of pressure traces and chemiluminescence emission for mixture no. 4; Experimental: RCEM (pressure), PMT (emission); Simulations: Zhao [17] and LLNL [13-15] (pressure).

**Species Measurements**

Measurements of the exhaust gas composition were conducted using the previously described micro GC. These measurements were conducted without the rapid expansion mechanism, using the machine as conventional RCM. The micro GC was calibrated for the following species: $CO_2$, $C_2H_2$, $C_2H_4$, $C_2H_6$, $C_2H_5OC_2H5$, $H_2$, $O_2$, $N_2$, $CH_4$, CO, $CH_3OCH_3$, $CH_3OH$, $C_2H_5OH$, and $C_3H_6O$. Measurements of the exhaust gas composition were performed for the investigated temperature range of mixture no. 2 and 4. Since there was almost no influence of the temperature at TDC on the species composition, the results of only one measurement are shown in figure 9 and 10.

Simulations were again conducted using a homogeneous reactor model with the mechanisms developed by LLNL [13-15] and Zhao et al. [17]. After ignition occurred in the simulations, the mixture was cooled to the pressure and temperature obtained experimentally during analysis. This simple homogeneous model was used to obtain at least some preliminary information about the theoretically expected chemical composition of exhaust gas. Species with a mole fraction below the absolute tolerances of the simulation are not shown in figure 9 and 10.

In contrast to the simulations a small amount of oxygen and dimethyl ether (DME) was observed experimentally (figure 9). These small amounts of unburned mixture are probably from the colder parts in the reaction chamber (crevice and thermal boundary layer) which do not undergo any reaction or react only partially. These were not taken into account in the simulations; the comparisons are to be interpreted as more qualitative. The presence of these species can

deliver valuable information about the fractional part of the cylinder load trapped in cold boundary layers and crevices.

An agreement between the experiment and the simulations with the Chaos mechanism is observed for the amount of $CO_2$ in both mixtures. The simulation with the LLNL-mechanism results in slightly higher values of $CO_2$, which is likely caused by the full conversion of DME. Both mechanisms predict the amount of carbon monoxide for the rich mixture well. However, for the stoichiometric mixture a higher value of carbon monoxide was observed experimentally.

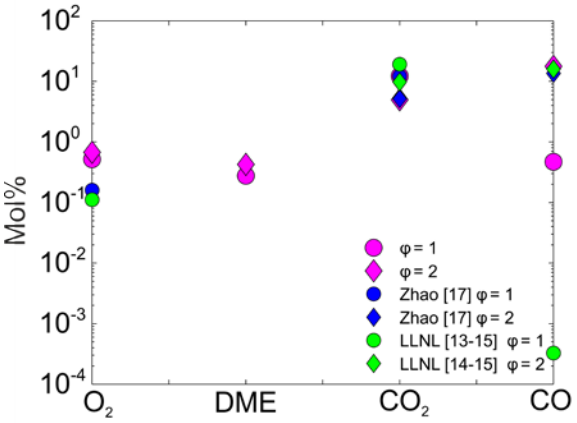


Fig. 9 Comparison of the measured and simulated species concentration in the exhaust gas for mixture 2 and 4. Note that the deviations are likely due to the simple homogeneous reactor model and do not allow conclusion of the mechanism accuracy.

Figure 10 shows, that there is a greater difference in the amount of hydrogen in the exhaust gas between simulations and experiment. Especially for the rich mixture, the difference is significant. In the experiments a mole fraction of 10% a ten times higher value as with the LLNL [13-15] mechanism was observed. In comparison with the Zhao et al. [17] mechanism the difference was even greater.

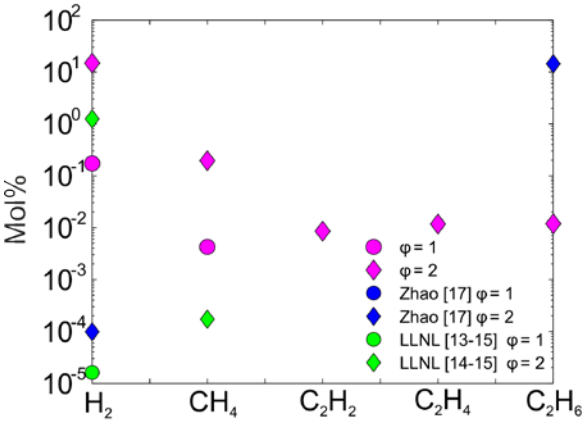


Fig. 10 Comparison of the measured and simulated species concentration in the exhaust gas for mixture 2 and 4. Note that the deviations are likely due to the simple homogeneous reactor model and do not allow conclusion of the mechanism accuracy.

For the detectable $C_1$ and $C_2$-species the results also diverge. The $C_2$-species could be detected in the exhaust gas of the experiments for the rich mixture (no. 4). In the exhaust gas of the simulation with the Zhao mechanism just $C_2H_6$ was observed in a considerable amount. However, this amount is much higher compared to the experiments. No considerable amount of the $C_2$-species was predicted by the model with the LLNL-mechanism. For the rich mixture methane was observed with a lower mole fraction as in the experiments.

**Conclusion**

The revised RCM was extended by a mechanism for rapid expansion of the test gas, allowing to stimulate and freeze chemical reactions in a controlled compression-expansions time history. A good repeatability of the experiments is derived by the new driving concept. Furthermore, a new measurement channel was added to the experimental setup, providing detailed ex-situ chemical analysis of gas samples extracted from the in-cylinder mixture with a GC.

To test the revised experimental setup, measurements of ignition delay times and chemical composition in DME-air-mixtures were conducted. Ignition delay times were compared to some of the experimental data available from [12-21].

An overall good agreement was observed. In the current study ignition delay times were slightly faster at extreme conditions, like very fast ignition delay times or highly diluted mixtures.

A comparison with the two reaction mechanisms developed by LLNL [13-15] and Zhao et al [17] were conducted for mixtures with $\phi = 1$ and $\phi = 2$. A good agreement for the slope of the ignition delay time vs. the inverse temperature was observed. The Zhao mechanism predicted the ignition delay times of this study somewhat more precisely than the LLNL mechanism.

Additionally the exhaust gas composition was compared between a simple model using the two reaction mechanisms and the experiment. The effect of the crevice and the boundary layer on the species composition in the exhaust can be seen by the little amount of unburned educts. A good agreement in the comparison was observed for carbon dioxide and for carbon monoxide in the rich mixture. The model predicts too low amounts of hydrogen and of $C_2$-species, except for ethane. In the simulation of the rich mixture with the Zhao et al. [17] mechanism a higher amount of ethane was observed compared to the experiment.

**Outlook**

As it can be seen in the figures 3, the revised RCM setup shows a good shot-to-shot repeatability. However, the pressure traces (also in figure 7 and 8) show a slight oscillations after the piston reaches TDC. Due to the relatively short stroke length, small motions of the piston result in noticeable pressure variations. In future work, the piston will be damped to reduce this oscillation in future.

The rapid expansion mechanism of the revised experimental setup allows to reduce quickly pressure and temperature in the mixture in a controlled manner as seen in figure 3. By applying the expansion before the final ignition takes place, the chemical composition of quenched samples from the partially reacted in-cylinder mixture will be analyzed, providing additional data for mechanism development and validation.

**Acknowledgements**

Financial support by the Deutsche Forschungsgemeinschaft within the framework of the DFG research unit FOR 1993 'Multi-functional conversion of chemical species and energy' is gratefully acknowledged.

**References**

[1] J. C. Livengood, W. A. Leary, Indust. and Engineering Chem. 43 (1951) 2797-2805
[2] R. Minetti, M. Ribaucour, M. Carlier, L R. Sochet, Combustion and Science Technology 113(1996) 179-192.
[3] S.M. Gallagher, H.J. Curran, W.K. Metcalfe , D. Healy, J.M. Simmie, G. Bourque, Combustion and Flame 153 (2008) 316–333.
[4] G. Mittal, C.J. Sung, Combustion Science and Technology 179(2007) 497-530.
[5] M. T. Donovan, X. He, B. T. Zigler, T.R. Palmer, M.S. Wooldridge, A. Atreya, Combustion and Flame 137 (2004) 351-365.
[6] D. Lee, S. Hochgreb, Combustion and Flame 114(1998) 531-545.
[7] M. Werler, L.R. Cancino, R. Schiessl, U. Maas, C. Schulz, M. Fikri, Proc. of the Comb. Inst. 35 (2015) 259-266.
[8] B.M. Gauthier, D.F. Davidson, R.K. Hanson, Combustion and Flame 139 (2004) 300-311.
[9] J.M. Simmie, Progress in Energy and Combustion Science 29 (2003) 599-634.
[10] M. H. Morsy, Fuel 86 (2007) 533-540
[11] T. A. Semelsberger, R. L. Borup, H. L. Greene, J. Power Sources. 156 (2006) 497-511
[12] P. Dagaut, J.-C. Boettner, M. Cathonnet; 26th (Int.) Symp. Comb. (1996) 627-632
[13] S. L. Fischer, F. L. Dryer, H. J. Curran, Int. J. Chem. Kinet 32 (2000) 713–740
[14] H. J. Curran, S. L. Fischer, F. L. Dryer, Int. J. Chem. Kinet 32 (2000) 741–759
[15] E. W. Kaiser, T. J. Wallington, M. D. Hurley, J. Platz, H. J. Curran, W. J. Pitz, C. K. Westbrook J. Phys. Chem 35 (2000) 8194-8206
[16] U. Pfahl, K. Fiewieger, G. Adomeit, 26th Symp. (Int.) Comb. (1996) 781-789
[17] Z. Zhao, M. Chaos, A. Kazakov, F. L. Dryer, Int. J. Chem. Kin 40 (2008) 1-18
[18] G. Mittal, M. Chaos, C.-J. Sung, F. L. Dryer, Fuel Processing Technology 89 (2008) 1244-1254
[19] U. Burke, K.P. Somers, P. O'Toole, C.M. Zinner, N. Marquet, G. Bourque, E.L. Petersen, W.K. Metcalfe, Z. Serinyel, H.J. Curran Combustion and Flame 162 (2015) 315–330
[20] R.D. Cook, D.F. Davidson, R.K. Hanson, Proc. of the Comb. Inst. 32 (2009) 189-196
[21] J. Zhang, E. Hu, L. Pan, Z. Zhang, Z. Huang, Energy and Fuels 27 (2013) 6247-6254